Complete ductility in NdFeB-type alloys using the Hydrogen Ductilisation Process (HyDP)

Brooks, Oliver; Walton, Allan; Zhou, Wei; Brown, David; Harris, Ivor

DOI:
10.1016/j.actamat.2018.04.055

Document Version
Peer reviewed version

Citation for published version (Harvard):
Brooks, O, Walton, A, Zhou, W, Brown, D & Harris, I 2018, 'Complete ductility in NdFeB-type alloys using the Hydrogen Ductilisation Process (HyDP)', *Acta Materialia*, vol. 155, pp. 268-278. https://doi.org/10.1016/j.actamat.2018.04.055

Accepted Manuscript

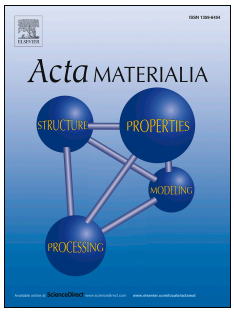

Complete ductility in NdFeB-type alloys using the Hydrogen Ductilisation Process (HyDP)

O. Brooks, A. Walton, W. Zhou, D. Brown, I.R. Harris

PII: S1359-6454(18)30332-X

DOI: 10.1016/j.actamat.2018.04.055

Reference: AM 14543

To appear in: *Acta Materialia*

Received Date: 5 January 2018

Revised Date: 14 April 2018

Accepted Date: 25 April 2018

Please cite this article as: O. Brooks, A. Walton, W. Zhou, D. Brown, I.R. Harris, Complete ductility in NdFeB-type alloys using the Hydrogen Ductilisation Process (HyDP), *Acta Materialia* (2018), doi: 10.1016/j.actamat.2018.04.055.

$$Nd_2Fe_{14}B + 2H_2 \rightleftharpoons 2NdH_2 + Fe_2B + 12\alpha Fe$$

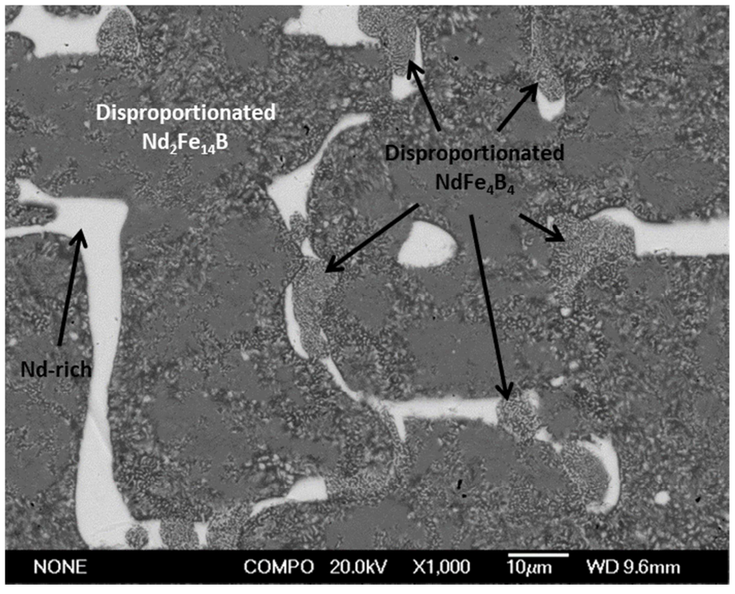

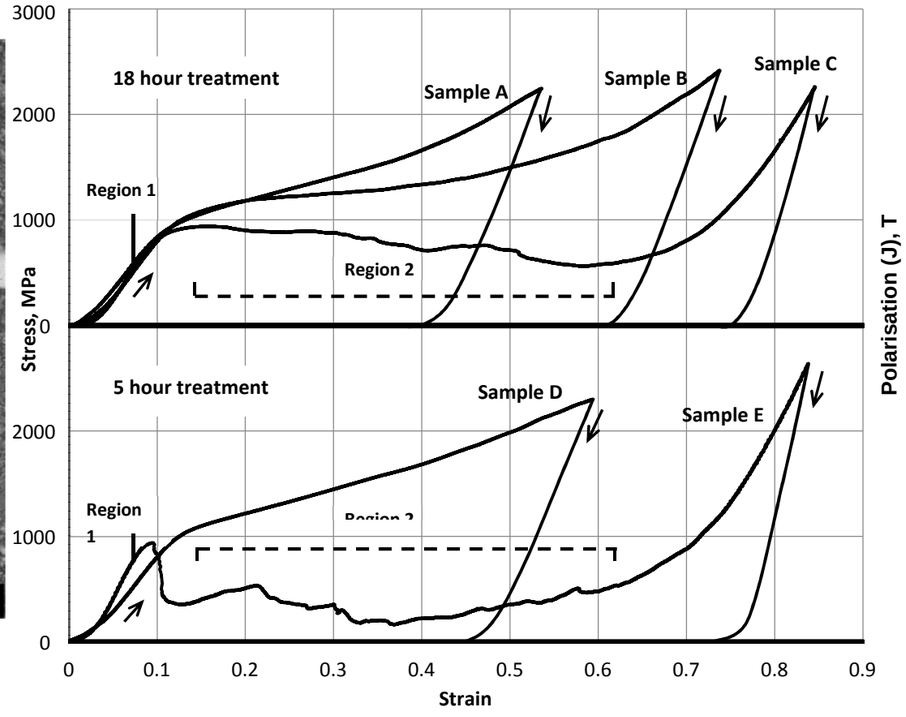

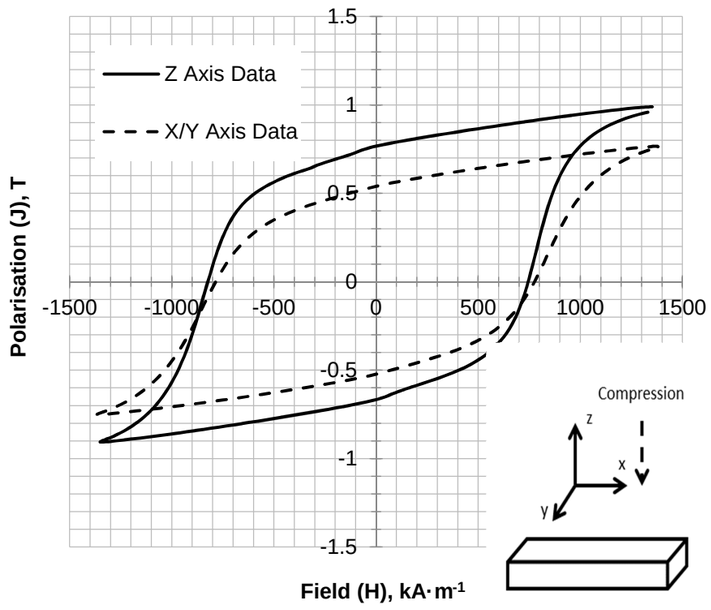

Complete ductility in NdFeB-type alloys using the Hydrogen Ductilisation Process (HyDP)

O. Brooks [a]*, A. Walton [a], W. Zhou [a], D. Brown [b] and I.R. Harris [a].

[a]School of Metallurgy and Materials, College of Science and Engineering, University of Birmingham, B15 2TT, UK.

[b]SG Technologies Limited, 85 Ferry Ln, Rainham RM13 9YH, UK

*Corresponding Author email: O.P.Brooks@bham.ac.uk

Abstract

The work outlined in this paper demonstrates significant improvements in ductility during the Hydrogen Ductilisation Process (HyDP) [1] of a Neomax-type alloy and, for the first time, complete ductility of a sub-stoichiometric alloy. In previous studies, the uniformity of the ductilisation transformation was limited by the presence of the $NdFe_4B_4$ phase not undergoing complete disproportionation, which left extremely brittle, micron-scale islands in a highly ductile disproportionated matrix. The present works investigated the influence of a significantly longer (18 h) hydrogen treatment of the Neomax-type alloy to observe whether the completely disproportionated $NdFe_4B_4$ phase is as ductile as the disproportionated matrix. It has been observed that, when the $NdFe_4B_4$ phase is completely disproportionated, it exhibits similar ductility to that of the disproportionated matrix, showing no sign of cracking under a compressive load. However, inhomogeneity in the book mould material leads to varying quantities of $NdFe_4B_4$ phase and thus, varying levels of disproportionation. Despite this, significant improvements were observed in the mechanical behaviour of the Neomax-type alloy. The longer disproportionation treatment also results in larger grains and thus, a lower final coercivity in the recombined state than that of the previous 5 h treatment. For comparison, the mechanical behaviour of a sub-stoichiometric alloy, which did not contain any $NdFe_4B_4$ phase, has also been studied. The compression behaviour of this sub-stoichiometric alloy in the disproportionated state was found to be completely ductile. It is clear from this work that it is possible to create a completely ductile NdFeB

material directly from the solid cast alloy which, in the future, could have significant implications for NdFeB magnet production.

1 Introduction

It has been shown previously by the authors that it is possible to change the extremely brittle cast NdFeB alloys consisting of the $Nd_2Fe_{14}B$ phase, a Nd-rich eutectic and the $NdFe_4B_4$ phase (approximate formula) [2] into an almost fully ductile mixture, which can be deformed significantly at room temperature, by first employing the high temperature solid-hydrogenation-disproportionation (s-HD) reaction, in a process which has been termed the *Hydrogen Ductilisation Process* (HyDP) [1]. During the solid-hydrogenation-disproportionation-desorption-recombination (s-HDDR) process [3], the Neomax-type ($Nd_{15}Fe_{77}B_8$) composition has been heated to >650 °C under vacuum and hydrogen is then introduced slowly, thus, causing the material to disproportionate progressively into a nanocrystalline mixture of NdH_2, Fe_2B and α-Fe (Equation 1) whilst avoiding the room temperature hydrogen decrepitation process. By maintaining an elevated temperature and by reducing progressively the hydrogen pressure, it is then possible to desorb the hydrogen, thus causing the disproportionated mixture to recombine into $Nd_2Fe_{14}B$ but now with a much finer, submicron grain size [4].

Equation 1

$$Nd_2Fe_{14}B + 2H_2 \rightleftharpoons 2NdH_2 + Fe_2B + 12\alpha Fe$$

The previous studies [1] have shown that, by halting the reaction in the disproportionated state, where there is a high percentage of α-Fe (see Equation 1), it is possible to deform the solid mixture, whilst maintaining a solid form, and then recombining the deformed mixture but now with a submicron grain size [1]. Furthermore, it has been found that appropriate deformation and desorption of the disproportionated state produced a degree of anisotropy in the recombined material. In this paper, an improved recombination procedure is outlined for the 5 h hydrogen treated Neomax-type which serves to improve the coercivity, as shown in Figure 2.

These studies involved work with the Neomax-type book mould cast (BMC) material which contained a minority $NdFe_4B_4$ phase [2] and it has been shown clearly that this phase also disproportionated but at

a significantly slower rate than that of the $Nd_2Fe_{14}B$ [5]. In the previous work [1], the Neomax-type material was maintained at 915 °C and 1200 mbar for 5 h, which was found to be sufficient to fully disproportionate the $Nd_2Fe_{14}B$ phase but only produced a partial decomposition of the $NdFe_4B_4$ phase. During the compression trials, the remaining, unreacted $NdFe_4B_4$ phase was shown to fracture producing fluctuations in the stress-strain measurements and reducing the density in both the disproportionated and recombined states.

One of the main aims of the present work was to increase the proportion of disproportionated $NdFe_4B_4$ phase by employing an increased s-HD hold time in the Neomax-type material, and studying the influence this treatment has on the mechanical properties, densities and subsequent magnetic properties. If it can be shown that the disproportionated $NdFe_4B_4$ demonstrates similar mechanical behaviour to that of the disproportionated $Nd_2Fe_{14}B$ phase then it should be possible to produce a fully ductile material, which can be shaped in this condition and then the hydrogen removed at a later date. Such a route could have significant advantages over primary production of fully dense sintered NdFeB magnets.

2 Experimental Work

The present studies employ two BMC alloys. The first being the Neomax-type BMC material of composition $Nd_{15}Fe_{77}B_8$ (provided by Less Common Metals (LCM UK)) and closely similar to that studied in the previous work [1]. In the initial BMC condition, this alloy contains $Nd_2Fe_{14}B$, Nd-rich material and $NdFe_4B_4$ confined predominantly to the grain boundaries [1, 6]. The second alloy is a sub-stoichiometric material with composition $Nd_{10.46}Pr_{3.43}Fe_{73.73}Co_{6.67}B_{5.12}Ga_{0.59}$ (provided by MagneQuench). This Fe-rich composition is employed in the cast condition and, in the current studies, the main interest of this material is that this particular alloy avoids completely the formation of the $NdFe_4B_4$ phase. This alloy has been produced by MagneQuench as the basis of an exchange enhanced, melt spun alloy that is the subject of a separate publication [7]. In the present work, this alloy has been employed strictly as a comparison for the compression behaviour compared with that of the

Neomax-type composition, as it does not contain the $NdFe_4B_4$ phase. The presence of excess iron confines its magnetic interest to that of the exchange-enhanced, melt-spun state.

Using spark erosion, these materials were either cut into cylinders, of ~9.5 mm diameter and ~5 mm height, or into cubes, of ~5x5x5 mm, as this technique limited the oxidation process which previous work [8] has shown, can have a significant influence on the disproportionation reaction.

As outlined first in 1995 by the resistivity studies of Gutfleisch and Harris [3], to produce fully disproportionated material the solid disproportionation reaction was employed using the same conditions as those adopted in the previous studies [1]. This involved heating the particular NdFeB alloy under vacuum, to 915 °C, and then introducing slowly, hydrogen to a pressure of 1200 mbar, in order to achieve 100% disproportionation, without decrepitation.

In the previous studies, for a Neomax-type cube sample (~25 mm^3) at 915 °C, SEM and XRD studies revealed that a period of around 5 h was sufficient to achieve 100% disproportionation of the matrix $Nd_2Fe_{14}B$ phase but only partially in the case of $NdFe_4B_4$ [1]. For the purpose of the present study, a set of Neomax-type samples were subject to the s-HD stage [3] for a longer period of 18 h in order to study the influence on the extent of the disproportionation of the $NdFe_4B_4$ phase and the subsequent change in the mechanical properties. It has been observed previously that the cracking of this phase during deformation has a profound influence on the compressive behaviour [1].

In order to maintain the disproportionated state the material was cooled rapidly in hydrogen. Figure 1 shows a schematic representation of the change of hydrogen pressure and temperature vs. time for both the 18 h and 5 h treatments. The formation of the more reactive $NdH_{2.7}$ component was avoided by partially degassing the material (after quickly cooling in hydrogen) up to 350 °C under vacuum.

In order to relate the mechanical behaviour to possible changes in the microstructure and to examine the fine structure of the disproportionated material both before and after compression, Jeol 6060 and Jeol 7000 scanning electron microscopes (SEMs) were employed (in the backscattered mode), using a

20 kV accelerating voltage. Some compositional analysis was also carried out using the EDX facilities on both microscopes.

As in the previous studies [1], detailed compression trials were carried out on an ESH 200 kN servo hydraulic mechanical press which allowed readings of both the force applied and the displacement to be measured, so that details of the mechanical behaviour of the particular samples could be determined. In this study, the change in cross sectional area during compression has not been taken into consideration and thus, the well-established "engineering" stress/strain units are employed. All compression trials have been performed in air.

Density measurements were calculated using the Archimedes principle. Samples were weighed in air and in a liquid of a known density (in this case diethyl phthalate).

A Lakeshore, vibrating sample magnetometer (VSM), capable of measurements up to a field of 2 T, was employed to measure the magnetic properties of the samples both before and after the compression trials at room temperature and after the subsequent recombination process. Self-demagnetisation factors have been taken into consideration with all the measurements.

3 Results

3.1 5 h disproportionated Neomax-type BMC

In the previous publication [1] it was shown that in BMC Neomax-type material, a 5 h hydrogen disproportionation was sufficient to disproportionate fully the matrix $Nd_2Fe_{14}B$ phase but only partially the $NdFe_4B_4$ phase, as shown in Figure 2(a).

Figure 2(a) shows a large area of unreacted $NdFe_4B_4$ phase (B) surrounded by Nd-rich material (A) and disproportionated $Nd_2Fe_{14}B$ (C). As reported previously [9], disproportionation of the $Nd_2Fe_{14}B$ phase occurs, initially at the interfacial regions and thus the degree of coarsening of the disproportionated mixture varies throughout the sample. As shown previously [1], there is evidence of the onset of disproportionation of the $NdFe_4B_4$ (B) phase (indicated by the arrow), but in this sample the phase remained largely unreacted. Previous work has shown that, it is possible to propagate this reaction

further with longer hold times and higher hydrogen pressures [5]. In this work, it has been shown that even with some brittle $NdFe_4B_4$ present in the material, it is possible to achieve appreciable coercivities and anisotropy in the Neomax-type alloys after 5 hours of hydrogen disproportionation (Figure 2(b)). The coercivity was shown to be 824 $kA \cdot m^{-1}$ and the remanence in the easy direction was 770 mT. In this case the conditions for recombination of this sample were altered from previous work [1] by first heating the pressed sample in 350 mbar of hydrogen up to 850 °C and then reducing the pressure by 100 $mbar \cdot min^{-1}$ to rotary pressure, then holding for 15 mins before cooling rapidly. This allowed for a more controlled recombination process and thus, to an improved coercivity compared to that reported in the previous work [1]. There were some indications of alignment in the material, with an easy-axis in the z-direction (pressing direction); this direction can be seen again in Figure 6(a). In comparison, conventional sintered magnets with a similar composition to that used here have typically, a coercivity of 800-1000 $kA \cdot m^{-1}$ and a remanence of 1200 mT [10, 11].

3.2 18 hour Disproportionated Neomax-type BMC and 5 hour Disproportionated Sub-stoichiometric BMC

A cube (~25 mm^3) of Neomax-type material, identical with that used in previous work [1], was taken and subject to hydrogen disproportionation for an extended period of 18 hours. A cube of sub-stoichiometric material was also subject to hydrogen disproportionation for 5 hours.

Figure 3 show the microstructure of the Neomax-type material after the 18 h treatment at 915 °C with an ambient pressure of 1200 mbar of hydrogen, prior to compression. Large regions of neodymium-rich material can be seen throughout but appeared to exhibit no general texture or shape in this undeformed sample. It can be observed that the matrix, $Nd_2Fe_{14}B$ phase has been disproportionated completely and that at the interfaces between the grain-boundary and $Nd_2Fe_{14}B$, where the disproportionation reaction initiates, the mixture of NdH_2, Fe_2B and Fe is now coarser than that observed for the previous 5 h s-HD treatment, in agreement with previous work [9].

As expected, after the 18 h treatment the alloy is observed to have undergone disproportionation to a far greater extent and in the case of the $NdFe_4B_4$ phase, where the phase is sparsely populated (Figure 3(a)), it has undergone complete disproportionation or, where the phase is more extensive (Figure 3(b)), it has undergone only partial disproportionation. These observations are consistent with the slower propagation of the disproportionation reaction in the $NdFe_4B_4$ phase, reported previously [5]. The disproportionated structure of the $NdFe_4B_4$ phase is much coarser than that of the initial $Nd_2Fe_{14}B$ disproportionated structure and of a similar scale to that seen in previous works [5] but now much more extensive. In both Figure 2(a) and Figure 3(b), the onset of disproportionation of $NdFe_4B_4$ appears at the interface with the matrix $Nd_2Fe_{14}B$ phase and not at the interface with the adjacent Nd-rich material. These images indicate that the 18 h, s-HD treatment is still insufficient to achieve complete disproportionation of the $NdFe_4B_4$ phase throughout the BMC Neomax-type material and to achieve complete disproportionation a significantly longer treatment will be required. These studies serve to show that importantly, the BMC material does not have a perfectly homogeneous microstructure. Figure 3(c) shows the microstructure of the disproportionated sub-stoichiometric material after a 5 h hydrogen treatment at 915 °C with an ambient hydrogen pressure of 1200 mbar. The disproportionated matrix can be observed alongside the Fe/Co-dendrites and the RE-rich material, with the notable absence of any brittle $NdFe_4B_4$ phase. As with the Neomax-type disproportionation, it can also be observed that the disproportionated microstructure is significantly coarser closer to the interfacial regions.

3.3 Compression trials

Cylinders of the Neomax-type material, ~9 mm diameter and ~5 mm height, were subject to the s-HD treatment for 18 h, cooled in hydrogen and then employed for compression trials at room temperature with a strain rate of 0.5 $mm \cdot min^{-1}$. The results for these experiments together with the previous measurements [1] are shown in Figure 4.

Figure 4(a) shows the stress-strain curves for three BMC Neomax-type samples (A, B and C) that have been subject to s-HD for 18 h, and Figure 4(b) shows the behaviour of the 5 h hydrogen treated samples; one sub-stoichiometric sample (D) (which has no $NdFe_4B_4$ phase present but a significant proportion of Fe dendrites), and one sample (E) from the previous work [1] which is known to contain a high proportion of regions of unreacted $NdFe_4B_4$ phase. Previously, it has been suggested that the almost 50% reduction in stress after the pseudo elastic region (region 1) and subsequent fluctuations (region 2) observed in the 5 h treated Neomax-type sample (E), were related to the fracturing of the unreacted, brittle $NdFe_4B_4$ phase during pressing [1]. Figure 4(b) shows that, when no $NdFe_4B_4$ phase is present in the material, as in sample D, then no reduction in stress is observed after region 1 and the subsequent fluctuations (region 2) observed in sample E are completely absent.

In Figure 4(a), the evidence of fluctuations (region 2) observed in sample E is much reduced (samples B and C) or almost completely eliminated (sample A). Sample A shows a curve that resembles closely that of sample D, with no reduction in stress after region 1 and only minor fluctuations observed in region 2. There are some differences in the plastic deformation region between these two curves (region 2) which are likely to be due to variations in the initial microstructures (i.e. the Fe dendrites present in D but not in the other).

Sample B and C also do not exhibit the same reduction in stress after region 1, observed in sample E. However, when compared with sample A they exhibit significant increases in fluctuation within region 2 which would suggest a brittle phase is still present. As will be shown later, the variations in region 2 between samples A, B and C can be attributed to variation in the size of $NdFe_4B_4$ phase present in each sample.

Region 1 of samples A, B, C and D exhibit similar gradients and yield points (~900-1000 MPa) suggesting a similar elastic behaviour. However, the gradient observed in these regions is significantly different to that observed in sample E, suggesting that the removal of the brittle $NdFe_4B_4$ phase has an

influence on the elastic behaviour of these materials. These variations in elastic behaviour will be the subject of future publications.

Sample A and D exhibit no signs of any material break-off during compression and no fluctuations in the stress during compression. The other two samples (B and C) both exhibited a small amount of material break-off after the compression trials.

It is important to note that all the Neomax-type samples were selected from similar regions of the BMC material but there are variations in the microstructure of the BMC material caused by inhomogeneous cooling during processing, so that, certain areas may have more $NdFe_4B_4$ phase present than in others. The behaviours shown in Figure 4 and the disproportionated areas shown in Figure 3, indicate clearly that, increasing the disproportionation time goes a long way to removing the fluctuations caused by the presence of undisproportionated, brittle $NdFe_4B_4$ phase and that the disproportionated state is much more ductile. However, the inhomogeneity in the BMC material has a marked effect on the disproportionation times required to remove completely these fluctuations by achieving complete disproportionation of the $NdFe_4B_4$ phase. As the brittle phases are removed and replaced with the much more ductile, disproportionated mixture, the material will require a significantly greater stress to plastically deform (as shown in Figure 4).

3.4 Pressed disproportionated SEM

As shown in Figure 5, the fine microstructure of the 18 h hydrogen treated samples employed in the compression trials shown in Figure 4 have been examined, after compression, using the SEM. In Figure 5, the images have been ordered in a way that the samples which exhibit the most fluctuations (C) in compression are shown first and the sample with the least fluctuations (D) shown last.

3.4.1 Sample C

Figure 5(a) & (b) show SEM images of areas of the cross section of sample C (compression trial shown in Figure 4(a)), and this sample exhibited the most fluctuations. Throughout the sample, large areas of cracked $NdFe_4B_4$ phase can be observed, appearing to vary between 20-50 μm in thickness and 100-

300 μm in length. Figure 5(a) reveals a fractured area of $NdFe_4B_4$ phase. Much of the phase has undergone disproportionation but, due the large area of this phase after the 18 h treatment, disproportionation was not complete. It can be seen that the cracking in the sample is isolated to the areas where disproportionation was incomplete, thus indicating that the disproportionated $NdFe_4B_4$ material is ductile and will deform under compression. Once again it can be seen that the disproportionation of the $NdFe_4B_4$ phase begins preferentially at the interface between the matrix $Nd_2Fe_{14}B$ and $NdFe_4B_4$ phases. There are also smaller areas of uncracked $NdFe_4B_4$ phase which have thicknesses between 10-20 μm and 100-300 μm in length. Figure 5(b) reveals an uncracked area, where the $NdFe_4B_4$ phase has undergone complete disproportionation. The $NdFe_4B_4$ disproportionated mixture remains completely intact after compression, further evidence that such a disproportionated mixture is ductile under the conditions employed in these studies.

The disproportionated $Nd_2Fe_{14}B$ phase and the Nd-rich phase in Figure 5(a) & (b) exhibit no evidence of cracking and the Nd-rich areas now appear to have become elongated in a direction perpendicular to the compression axis. This provides strong evidence for the ductility of the Nd-rich phase, when in the hydrogenated state.

3.4.2 Sample B

A cross section of sample B obtained after compression (Figure 4) is shown in Figure 5(c) & (d). This sample exhibits smaller areas of both the $NdFe_4B_4$ phase and Nd-rich material than in the previous sample (C) and this could account for the different compression behaviours between the two samples (C and B). Figure 5(c) shows the partially disproportionated $NdFe_4B_4$ phase in sample B and in this case, cracking is restricted to the unreacted $NdFe_4B_4$ phase and the disproportionated $NdFe_4B_4$ behaves in a similar manner to that observed in sample C. The major difference between Figure 5(c) and Figure 5(a) is the extent of the $NdFe_4B_4$ phase which, in sample B, appear to be <10 μm thick. Figure 5(d) shows an area of sample B with a mixture of fully disproportionated $NdFe_4B_4$ and matrix $Nd_2Fe_{14}B$ phases. Much as in sample C, after the compression trials, the disproportionated $Nd_2Fe_{14}B$

and $NdFe_4B_4$ mixtures remain uncracked and the areas of Nd-rich phase have become elongated in a direction perpendicular to compression axis, again confirming the ductility of this phase in the hydrogenated condition.

3.4.3 Sample A

A cross section of Sample A after the compression trial is shown in Figure 5(e) & (f). As with the previous samples, the disproportionated mixture remains uncracked and the Nd-rich areas have all become elongated perpendicular to the direction of the compression axis. Most of the $NdFe_4B_4$ phase has not cracked during compression as it has become fully disproportionated but there is still some cracking of the small amount of undisproportionated material.

In Figure 5(f) small cracked and undisproportionated areas of the $NdFe_4B_4$ phase can be seen alongside large, uncracked disproportionated $NdFe_4B_4$ material. This again suggests that the disproportionated phase is ductile and that, if the areas of unreacted $NdFe_4B_4$ phase are sufficiently small, then the fluctuations in compression stress-strain measurements can be minimised.

3.4.4 Sample D

Figure 5(g) shows a backscattered image of a cross section of a sample subject to a 5 h disproportionation treatment and subsequently compressed. The compression is from the top right and bottom left corners, as indicated on the micrograph. This material exhibits two major differences to that of the Neomax-type samples described earlier; the first is that no $NdFe_4B_4$ phase is present in this sample and the second is that Fe/Co dendrites are present throughout the sample, related to the exchange enhancement of this material in the melt spun condition [7]. It can be seen that the Fe/Co dendrites have begun to become elongated and to align perpendicular to the axis of compression. The regions of neodymium hydride in the material have also become deformed in the same direction as the Fe dendrites without any evidence of cracking, thus exhibiting extensive ductility.

Figure 5(h) shows the disproportionated mixture of the pressed sample D (sub-stoichiometric material). The microstructure produced by the 5 h disproportionation treatment is finer than that of the previous

materials (due to the lower reaction time) and remains intact with no evidence of cracking after compression. (This behaviour is confirmed by the density studies).

3.5 Density

Table 1 summarises the density values measured and the percentage change in density from the starting material for samples at various points during the processing steps described earlier. After hydrogen disproportionation there is a decrease in density for both the 5 h and 18 h samples from 7.391±0.014 g/cc to 7.163±0.011 g/cc and 7.125±0.009 g/cc, a 3.1-3.6% reduction, this is to be expected as the s-HD reaction results in an expansion of the material but adds little mass, with the maximum theoretical density of a single phase $Nd_2Fe_{14}B$ fully disproportionated material calculated to be 7.18 g/cc [12]. The density of the 18 h disproportionated sample is lower than that of the 5 h sample and this can be attributed to the greater degree of disproportionation of the $NdFe_4B_4$ phase in the latter condition. The sub-stoichiometric material also decreases in density by 5.9% after the hydrogen treatment from 7.628±0.006 g/cc to 7.181±0.002 g/cc.

Once pressed, both the 5 h and 18 h samples exhibit a significantly lower density but the 5 h sample loses a large overall percentage, dropping to 6.821±0.022 g/cc, a 4.6% decrease from the initial disproportionated state. This can be ascribed to the cracking of the greater amount of unreacted $NdFe_4B_4$ phase present in the 5 h hydrogen treatment than that of the 18 h. All of the Neomax-type 18 h disproportionated samples used in compression trials shown in Figure 4 have a decrease in density but the decrease varies from sample to sample, with the sample that produced the least fluctuations in the compression behaviour (Sample A) exhibiting the highest density of 6.912±0.003 g/cc, a 2.89% decrease from the disproportionated state, and the one exhibiting the most fluctuations (Sample C) exhibiting the lowest at 6.840±0.004 g/cc, a 3.87% decrease from the disproportionated state. All of the 18 h samples exhibited a significantly higher density that that of the compressed 5 h disproportionated Neomax-type samples and this can be ascribed to the higher percentage of disproportionated $NdFe_4B_4$ phase and thus, reduction in fractured material after compression. The variation in density in the 18 h

samples can be ascribed to the varying content of unreacted $NdFe_4B_4$ phase and thus, subsequent fracturing during compression.

Sample D also decreases in density from 7.181±0.002 g/cc to 7.146±0.004 g/cc after compression. This change in density of 0.46% is much lower than that of the Neomax-type samples and this can be attributed to the absence of the brittle $NdFe_4B_4$ phase.

Upon recombination, full density of the starting Neomax-type material (7.391±0.014 g/cc) is not achieved in either the pressed (7.195±0.005 g/cc) or non-pressed samples (7.191±0.003 g/cc). This can be ascribed partially to the cavitation which will form during recombination [3] , as can be observed in the later SEM images (Figure 7). However, this can also be ascribed to an incomplete recombination which leads to areas of the disproportionated mixture present within the microstructure, which is known to have a lower density than the $Nd_2Fe_{14}B$ phase [12].

For the compressed 5 h hydrogen treated material a more significant decrease in density (4.27%) was observed after the recombination procedure and this can be attributed to complete recombination and thus, a greater proportion of cavitation. The density of the pressed 5 h sub-stoichiometric material also does not fully recover after recombination and has a value of 7.318±0.006 g/cc, a decrease of 4.06% from the starting material. This can be ascribed to cavitation which will form during recombination [3], however it was also observed through SEM imaging that this material had not fully recombined under the same conditions employed for the 5 h hydrogen treated Neomax-type material. This SEM imaging will be part of a future investigation and is not included in this publication.

3.6 Magnetic measurements

The samples prepared for the VSM studies were in the form of 5 mm cubes, pressed at 5 t for 5 mins in a 10 mm diameter die set. This load over area equates to a stress of around 1900 MPa, similar to that employed in the compression trial shown in Figure 4.

A pressed and a non-pressed sample were placed back in the reaction vessel at a hydrogen pressure of 350 mbar, at room temperature, and subsequently heated to 850 °C. Once at temperature the

pressure of hydrogen was reduced so that desorption and recombination would occur. After a rotary pump vacuum (~10^{-2} mbar) was achieved, the samples were left for a further 15 mins to ensure complete recombination. This procedure was identical with that carried out on the previous 5 h reacted Neomax-type samples shown in Figure 2(b).

The pressed sample (used for the VSM measurements) on compression made contact with the side walls of the die. Initially a rectangular shape was cut and measured from a pressed and recombined sample, which included the sides which, on compression, made contact with the die wall. A 3-D representation of the compressed sample is shown in Figure 6(a) with the direction of compression. Figure 6(b) is a 2-D representation of the compressed sample where the dotted lines represent the sides which made contact with the die walls. This sample was then modified by removing any material which made contact with the die wall and measured a second time. All magnetic hysteresis loops which are shown have been correct for self-demagnetisation.

3.6.1 Initial VSM sample

Figure 6(c) shows the magnetic hysteresis produced for a sample, which includes the sides which have made contact with the die wall. The coercivity for this sample is consistently ~500 kA·m^{-1} in each direction but the remanence varies for each direction measured. In the y direction remanence is 550 mT, in the z direction it is 650 mT and in the x direction it is 730 mT. These measurements indicate a lower coercivity than that of the 5 h disproportionated pressed and recombined sample, shown in Figure 2(b), which exhibited a coercivity of ~820 kA·m^{-1}. In the 2nd quadrant of the hysteresis loops for the x and y directions the usual knee shape expected for ferromagnetic material is inverted. This behaviour is indicative of a material where recombination is incomplete.

3.6.2 Modified VSM sample (middle section)

The sample measured in Figure 6(c) was altered by removing around 1.5 mm from each end of the sample (3 mm total) in the x-direction.

Figure 6 (d) shows the hysteresis loop for this modified sample. There is a clear difference between the z and x/y direction. Coercivity remains similar in these directions but it is now reduced slightly (~410 $kA \cdot m^{-1}$) when compared with that shown in Figure 6(c). The remanence for the x and y directions are now the same ~550 mT and the z direction has increased to 710 mT. The x and y directions now show an almost identical trace, but both have the unusual knee shape in the 2nd quadrant which is not present in the z-direction. The precise cause of this phenomenon and its absence in the z-direction are unclear but as this is not present in fully recombined material observed in the previous work [1] and in Figure 2, then this could likely be ascribed to Fe present as the result of an incomplete recombination. As such, this unusual behaviour will be the subject of future investigation.

3.6.3 s-HDDR sample without pressing

Figure 6(e) shows the hysteresis loop for a cube of Neomax-type sample which had an 18 h s-HD treatment and was then cooled in hydrogen. The sample was then recombined under the same conditions as the previous sample but with no pressing (effectively a s-HDDR treatment with an intermediate cooling stage). This sample is completely isotropic and has a very low coercivity. This could be ascribed to an incomplete recombination however, as will be shown later, the incomplete recombination is far more extensive than the pressed samples. This aspect is being investigated further.

3.6.4 Sub-stoichiometric sample

The magnetic data for the pressed sub-stoichiometric alloy did not exhibit any significant coercivity, as expected from the high quantity of Fe/Co dendrites in the BMC alloy. In addition it was completely isotropic and as such has not been shown in this paper.

3.7 Recombined Microstructure

3.7.1 Pressed recombined 18 h hydrogen treated material

The disproportionated pressed and then recombined 18 h hydrogen treated Neomax-type material used in the VSM measurements was cross sectioned and imaged using the SEM, as shown in Figure 7.

Figure 7(a) shows a low magnification image of the pressed, fully recombined Neomax-type material used in the VSM measurement in Figure 6(d). Strips of dark cavitation can be observed in a direction perpendicular to that of the compression direction. These can be ascribed to cavitation which has formed from the Nd-strips, due to the redistribution of the aligned Nd-rich phase during recombination (see Figure 5) [3]. If the HyD process can be exploited in the production of magnets then it will probably be necessary to remove the cavitation by isostatic pressing or re-compressing the alloys in the disproportionated state thus, closing, at least partially, the cavitation. Alternatively, processing a low rare earth content alloy, would remove the large areas of Nd-rich grain boundary material and thus, avoid cavitation during the recombination, or subsequent additions of the Nd-rich phase, could fill the cavitation. However, it should be noted that using a low rare earth content alloy will introduce Fe dendrites into the BMC material and thus, will lower the coercivity. The efficiency of these steps can be determined by the precise density trials, as described earlier.

Towards the centre of the sample there is a large area which doesn't exhibit any cavitation and this would be consistent with an area of incomplete recombination.

Figure 7(b) shows an image of the area in Figure 7(a) which does not exhibit any cavitation and it appears that this area has not fully recombined with respect to the $NdFe_4B_4$ or the $Nd_2Fe_{14}B$ phase, (confirmed by EDX measurements). This is evident from the small areas of Fe (dark spots) which are present in the microstructure together with the coarse structure which is still present in the $NdFe_4B_4$ phase and the remaining Nd-rich phase. In this state, the disproportionated $NdFe_4B_4$ phase exhibits no evidence of fracturing, further suggesting that this is as ductile as the disproportionated $Nd_2Fe_{14}B$ mixture.

Figure 7(c) shows a magnified image of the areas of cavitation indicated by Figure 7(a); inside these areas there is the expected submicron grain structure. This structure does not appear to show any obvious grain orientation with respect to the direction of compression.

Figure 7(d) shows an area of complete recombination for both $NdFe_4B_4$ and for the $Nd_2Fe_{14}B$ phase, confirmed by EDX, where a region of $NdFe_4B_4$ separates two areas of $Nd_2Fe_{14}B$. The $NdFe_4B_4$ phase in the centre of the image exhibits a few minor cracks whereas the $Nd_2Fe_{14}B$ phase is fully dense.

Figure 7(e) shows another area of complete recombination. As with Figure 7(c), cavitation is present in the centre of the image and there is an area of $NdFe_4B_4$ phase, which has been confirmed by EDX, which has cracked and is surrounded by cavitation, indicating the original presence of the Nd-rich phase. This area of $NdFe_4B_4$ does not exhibit any evidence of disproportionation or recombination as has been seen in Figure 7(b) & (d), and has likely cracked during compression.

The fractured surface image shown in Figure 7(f) shows that, in the recombined material, there is a large variation in the grain size. The material exhibits many grains of submicron size but, there also exist several grains which are ~1-4 μm in size. These larger facetted grains can be ascribed to the presence of the coarse disproportionated microstructure, seen in earlier figures. It can be concluded that these larger grains will also have a negative impact on the final coercivity as they are larger than that of the single domain grains (300 nm).

3.7.2 s-HDDR sample with no compression

The s-HDDR 18 h disproportionated sample used for VSM measurements in Figure 6(e) was also examined using SEM imaging as shown in Figure 8.

The image shown in Figure 8(a) shows an area of a sample which has been recombined, under the same condition as the sample shown in Figure 7(a), but this time without any compression. None of the Nd-rich phase has redistributed and there is still evidence of disproportionation and hence incomplete recombination.

Figure 8(b) shows an area of the s-HDDR sample used for the VSM measurement which is consistent with the presence of the $Nd_2Fe_{14}B$ phase, confirmed by EDX analysis. The small black and white spots throughout the image have been confirmed by EDX to be small regions of α-Fe and Nd-rich material, and confirm the incomplete nature of the recombination process. However, the structure has been

altered slightly when compared with that shown in Figure 3(b). The presence of such quantities of Fe (dark phase) in the structure would limit the value of coercivity and this is consistent with the results from the VSM measurements shown in Figure 6(e).

Figure 8(c) again shows the structure of the incomplete recombination in the s-HDDR sample showing several areas of α-Fe and neodymium throughout the structure which vary in size up to ~3 μm. Figure 8(d) shows an area of $NdFe_4B_4$ phase where only partial disproportionation has occurred. As in Figure 7(b), the $NdFe_4B_4$ phase appears not to have completely recombined and this is consistent with the sluggish nature of this reaction. Due to the incomplete recombination of the surrounding $Nd_2Fe_{14}B$ phase, the Nd rich areas have not been redistributed, hence the absence of any cavitation as seen in the earlier images.

The images of the recombined samples show that, by compressing the samples, a faster recombination is possible and this can be ascribed partially at least to the change in the surface area and thickness of the sample. Due to the increase in the coarse disproportionated structure in the 18 h treated samples the same recombination conditions used for the 5 h disproportionated samples may not be suitable and a combination of a longer hold time under vacuum pressure and higher temperatures, may be required to achieve the optimal properties. This will be the subject of further investigation.

4 Conclusions

The work described in this paper has unequivocally demonstrated that the Hydrogen Ductilisation process (HyDP) can be used to achieve complete ductility in NdFeB alloys which do not contain any undisproportionated $NdFe_4B_4$ phase. The main findings of this investigation can be summarised as follows:

- The brittle nature of the $NdFe_4B_4$ phase observed previously in the 5 h hydrogen treated Neomax-type BMC material [1] can be significantly overcome by increasing the disproportionation time to 18 h, almost fully disproportionating the $NdFe_4B_4$ phase and in doing so creating an almost fully ductile NdFeB material prior to recombination.

- Complete ductility can be achieved by employing the 5 h hydrogen treatment on a sub-stoichiometric alloy, which avoids completely the formation of $NdFe_4B_4$ in the BMC condition. However, in the BMC condition this alloy contains Fe/Co dendrites which are detrimental to the magnetic properties of the recombined material.
- As expected, the 18 h hydrogen treatment produced a coarse disproportionated microstructure and thus, large grains in the recombined condition and hence much diminished magnetic properties [13]. The longer disproportionation hold time also led to a slower recombination and thus, the recombination conditions employed to fully recombine the 5 h hydrogen treated samples are not sufficient to fully recombine the 18 h treated samples.
- It was observed that the anisotropic behaviour of the recombined material changed significantly when the samples made contact with the die wall. This behaviour is akin to that of MQIII material formed during hot compression of melt spun material [14].

It is clear that the HyD process can produce a fully dense, fine grained, anisotropic NdFeB magnet directly from an NdFeB alloy by pressing. Although there are several challenges which need to be addressed, this process would offer clear advantages over the conventional sintered magnet production route, namely –

1. The HyD process may not require an inert atmosphere as the material does not have a high surface area.
2. A fine grain structure can be achieved (with suitable conditions) which if optimised could lead to very high coercivities.
3. This process would only require 4 process steps as opposed to 8-10 for sintered magnet production.
4. It may be possible to roll or extrude the material into sheets or rods without the production of waste material.

To date the best magnetic properties have been for a Neomax-type alloy pressed at 5 t with a coercivity of 824 $kA \cdot m^{-1}$ and a remanence of 770 mT. Although the coercivity is close to that expected for a

sintered magnet of a similar composition the remanence is significantly lower than that for a commercially produced sintered magnet based on the Neomax composition [10, 11]. In order to achieve a significantly higher $BH_{(max)}$, the $NdFe_4B_4$ phase would have to be removed to reduce cracking, the cavitation would have to be eliminated and a higher level of deformation would have to be achieved. All this is currently being investigated as part of further work. The fact that full ductility can be achieved in these materials may open the door to a suite of processing techniques moving forward.

5 Acknowledgements

Thanks to the Magnetic Materials group at University of Birmingham. In particular, to Andy Bradshaw, Richard Sheridan, Malik Degri and Vicky Mann. Also to Christian Jönsson for his assistance with the disproportionation trials. Warm thanks are also due to David Price for the invaluable help with the compression trails and to Professor Paul Bowen for the loan of compression equipment. David Kennedy is also gratefully acknowledged for very helpful discussions. Thanks also to MagneQuench and to Less Common Metals for supply of material. This work was supported by the UK EPSRC.

6 References

[1] O. Brooks, A. Walton, W. Zhou and I. Harris, The Hydrogen Ductilisation Process (HyDP) for shaping NdFeB magnets, Journal of Alloys and Compounds 703(2017)538–547

[2] D. Givord, J. M. Moreau and P. Tenaud, Nd7Fe18B18 (Nd1.11Fe4B4), a new nowotny-like phase. structural and magnetic properties, Solid State Communications 55(1985)303-306.

[3] O. Gutfleisch and I. R. Harris, In-situ electrical resistivity measurements: study of magnetic and phase transitions and solid-HDDR processes in Nd-Fe-B-type alloys, Journal of material science 30(1995)1397-1404

[4] R. Nakayama, T. Takeshita, M. Itakura, N. Kuwano and K. Oki, Magnetic properties and microstructures of the Nd-Fe-B magnet powder produced by hydrogen treatment, Journal of Applied Physics 70(1991)3770-3774

[5] V. Yartys, O. Gutfleisch and I. Harris, Hydrogen-induced phase and magnetic transformations in Nd1.1Fe4B4, Journal of Magnetism and Magnetic Materials, 157(1996)119-120

[6] M. Sagawa, S. Hirosawa, H. Yamamoto, S. Fujimura and Y. Matsuura, Nd–Fe–B Permanent Magnet Materials, Japanese Journal of Applied Physics 26(1987)785

[7] G. A. Zickler, J. Fidler, A. Asali, D. Brown and J. Bernardi, TEM/STEM study of rapidly quenched hard magnetic Nd-Fe-B ribbons, in European Microscopy Congress 2016: Proceedings, Lyon, 2016.

[8] R. Sheridan, A. Williams, I. Harris and A. Walton, Improved HDDR processing route for production of anisotropic powder from sintered NdFeB type magnets, Journal of Magnetism and Magnetic Materials 350(2014)114-118

[9] O. Gutfleisch, M. Matzinger, J. Fidler and I. Harris, Characterisation of solid-HDDR processed Nd16Fe76B8 alloys by means of electron microscopy, Journal of Magnetism and Magnetic Materials 147(1995)320-330

[10] O. Ragg and I. Harris, A study of the effects of Cu-addition on the annealing behavior and microstructures of Nd-Fe-B type sintered magnets, IEEE Transactions on Magnetics 29(1993)2758-2760

[11] H. Takiishi, L. Lima, I. Costa and R. Faria, The influence of process parameters and alloy structure on the magnetic properties of NdDyFeBNb HD sintered magnets, Journal of Materials Processing Technology 152(2004)1-8

[12] A. Williams, O. Gutfleisch and I. Harris, S-HDDR induced cavitation in NdFeB, Journal of Alloys and Compounds 232(1996)22-26

[13] S. Sugimoto, H. Nakamura, K. Kato, D. Book, T. Kagotoni, M. Okada and M. Homma, Effect of the disproportionation and recombination stages of the HDDR process on the inducement of anisotropy in Nd-Fe-B magnets, Journal of Alloys and Compounds 293-296(1999)862-867

[14] R. Lee, E. Brewer and N. Schaffel, Processing of Neodymium-Iron-Boron melt-spun ribbons to fully dense magnets, *IEEE Transactions on Magnetics* 21(1985)1958-1963

Sample	Density, g/cc	Error ±	% change from BMC condition
Start Neomax cast	7.391	0.014	N/A
Start sub-stoichiometric cast	7.628	0.006	N/A
Non-pressed disproportionated material			
5 h neomax	7.163	0.011	3.09%
18 h Neomax (Samples A, B and C)	7.125	0.009	3.59%
5 h sub-stoichiometric (Sample D)	7.181	0.002	5.85%
Maximum theoretical density of disproportionated material [12]	7.18	N/A	N/A
Pressed disproportionated material			
Neomax sample A after compression	6.912	0.003	6.48%
Neomax sample B after compression	6.881	0.004	6.90%
Neomax sample C after compression	6.840	0.004	7.46%
Sub-stoichiometric sample after compression (Sample D)	7.146	0.004	6.32%
Neomax 5 h disproportionation after compression	6.821	0.022	7.71%
Recombined material			
Neomax 18 h Disproportionation-recombined VSM sample	7.191	0.003	2.71%
Neomax 18 h Disproportionation-pressed-recombined VSM sample	7.195	0.005	2.65%
Neomax 5 h Disproportionation-pressed-recombined	7.076	0.011	4.27%
sub-stoichiometric 5 h Disproportionation-pressed-recombined	7.318	0.006	4.06%

Table 1 Densities for Neomax-type and sub-stoichiometric materials at various points through the HyD process

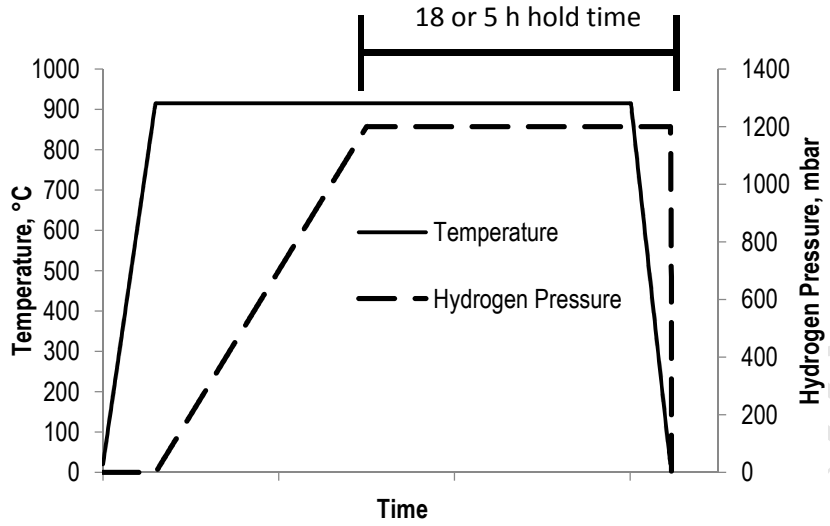

Figure 1 A schematic of the variation in Hydrogen Pressure and Temperature vs. Time during the disproportionation reaction

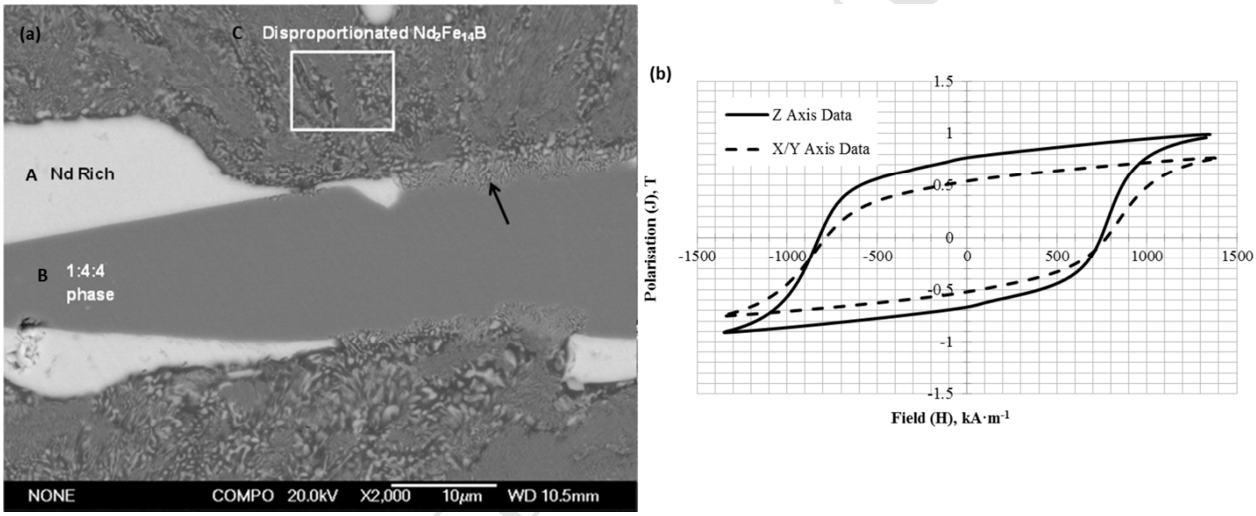

Figure 2 Previous studies [1] showing (a) backscattered SEM image of 5 h disproportionated Neomax-type material identifying partial disproportionation of the $NdFe_4B_4$ phase (see arrow), (b) VSM measurement of 5 h Neomax-type HyDP sample.

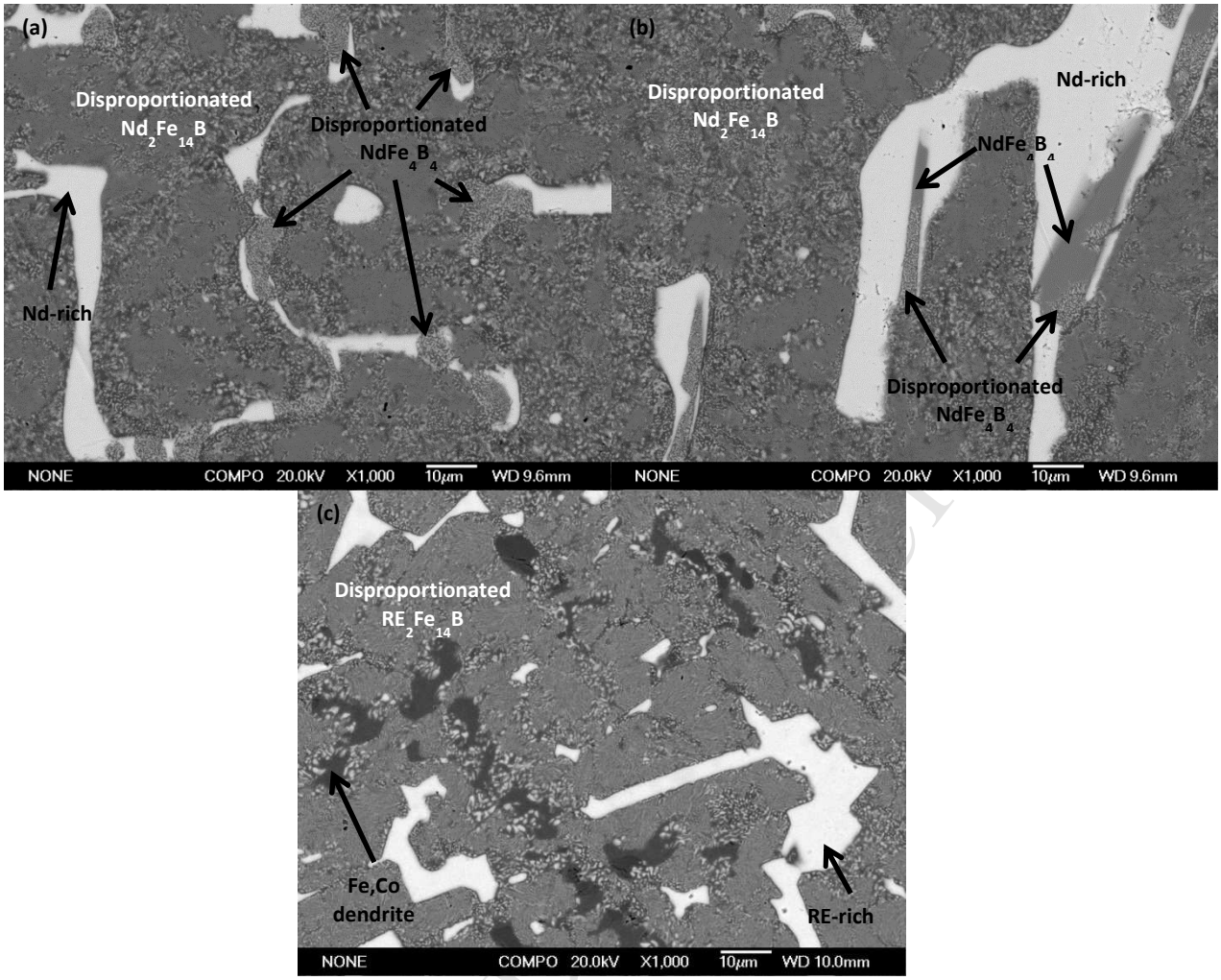

Figure 3 Backscattered SEM images of s-HD; (a) & (b) Neomax-type material after 18 h at 915 °C and 1200 mbar and (c) sub-stoichiometric material after 5 h at 915 °C and 1200 mbar.

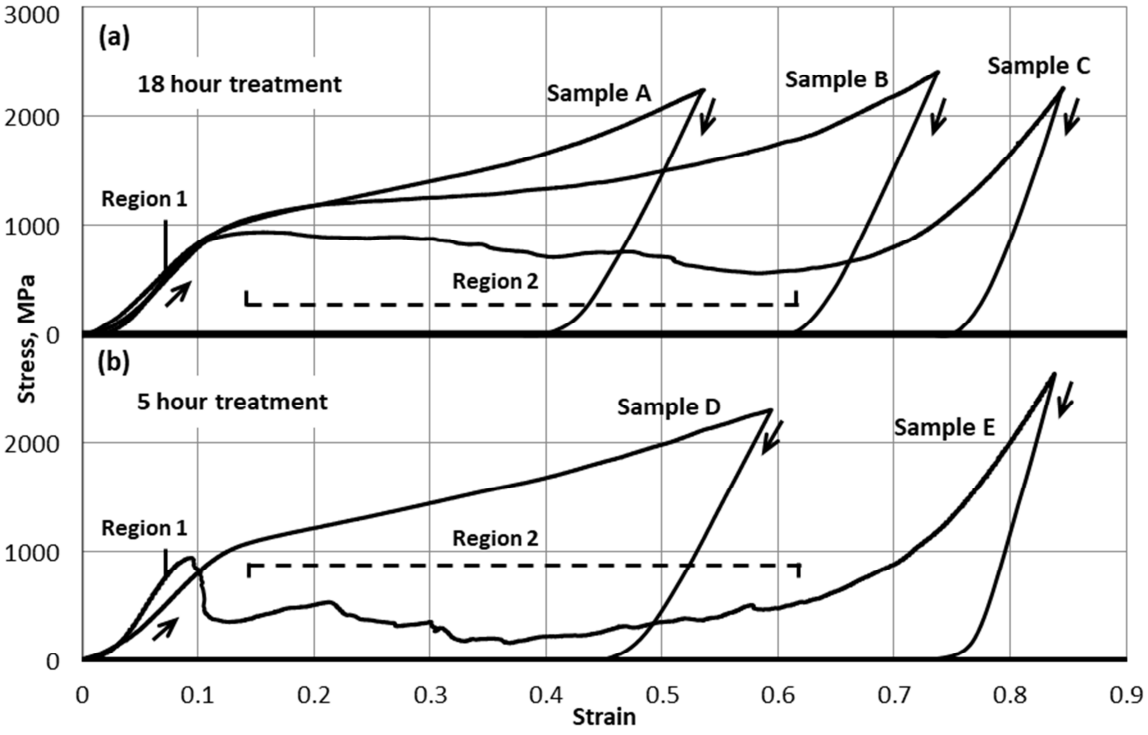

Figure 4 Stress-Strain curves: (a) 18 h hydrogen processed Neomax-type samples and (b) 5 h processed samples (sub-stoichiometric alloy (Sample D) and Neomax [1] (Sample E)), all with the strain rate of 0.5 mm·min^{-1}. Regions 1 and 2 representing the pseudo elastic and fluctuated plastic regions, respectively.

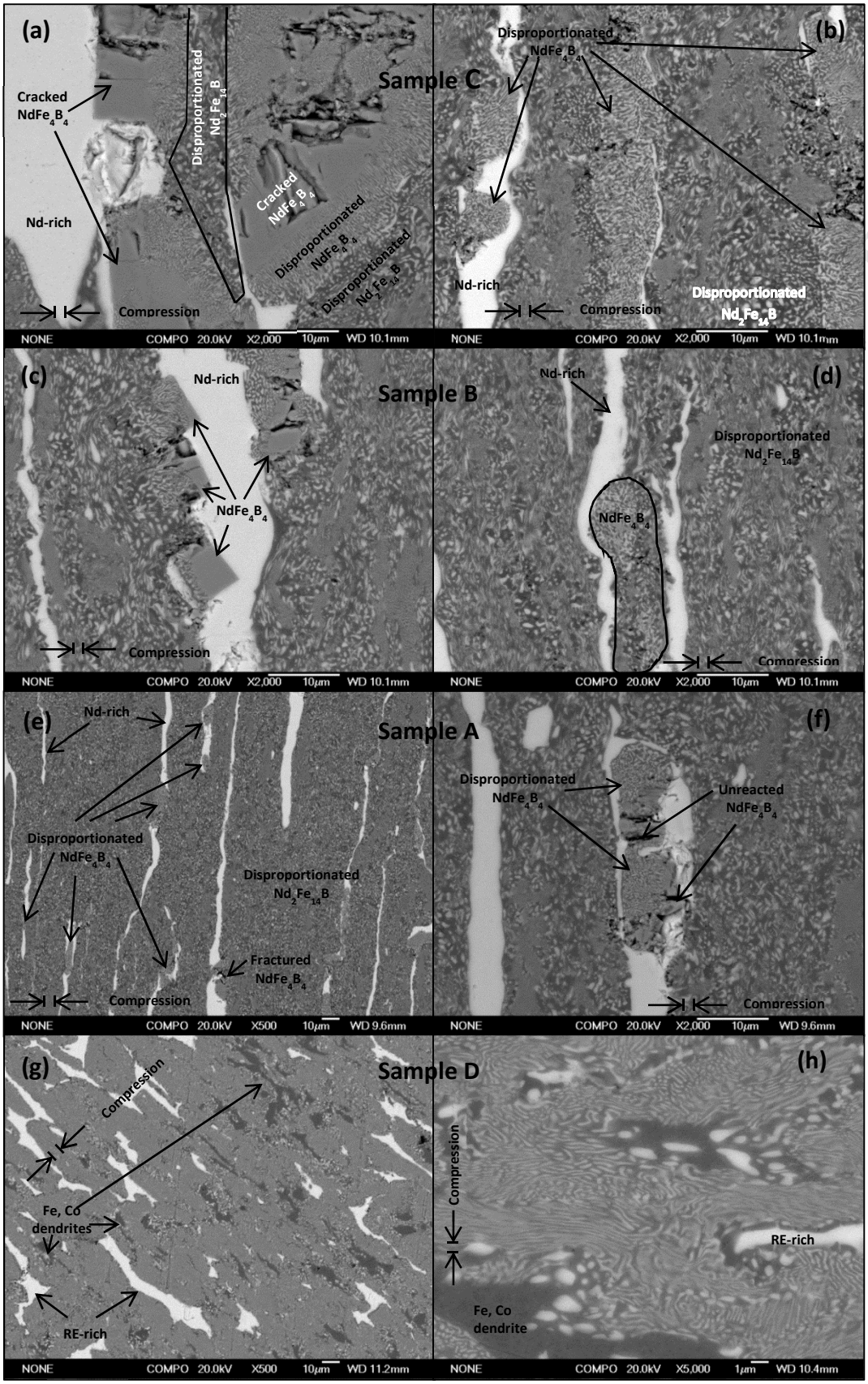

Figure 5 Backscattered SEM images of cross sections of samples after compression trial. (a)& (b) sample C, (c) & (d) sample B, (e) & (f) sample A and (g) & (h) Sub-stoichiometric sample.

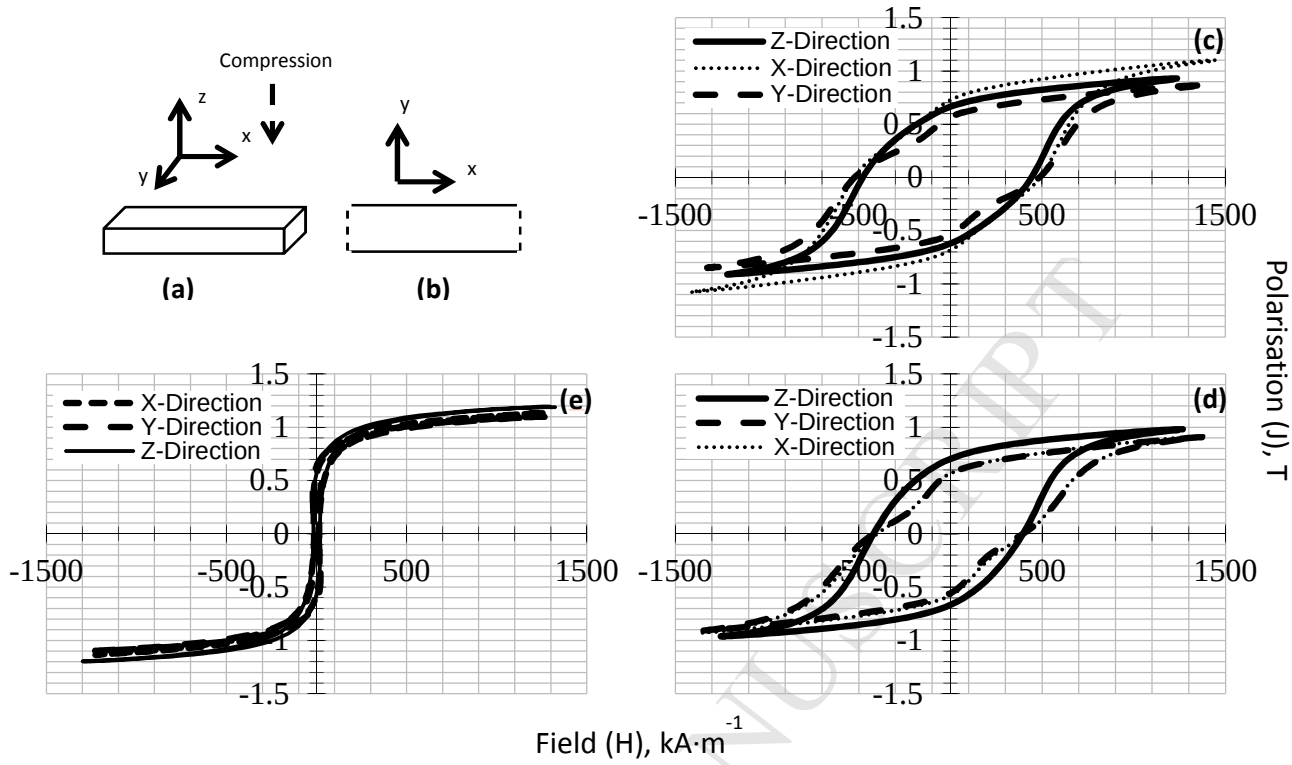

Figure 6 (a) 3-D representation of VSM sample, (b) Top down view of VSM sample with dashed lines to show sides which touch the die walls. VSM traces for an 18 h hydrogen processed HyDP Neomax-type sample; (c) full sample with dies wall contact, (d) middle section of the sample (e) s-HDDR cube without compression.

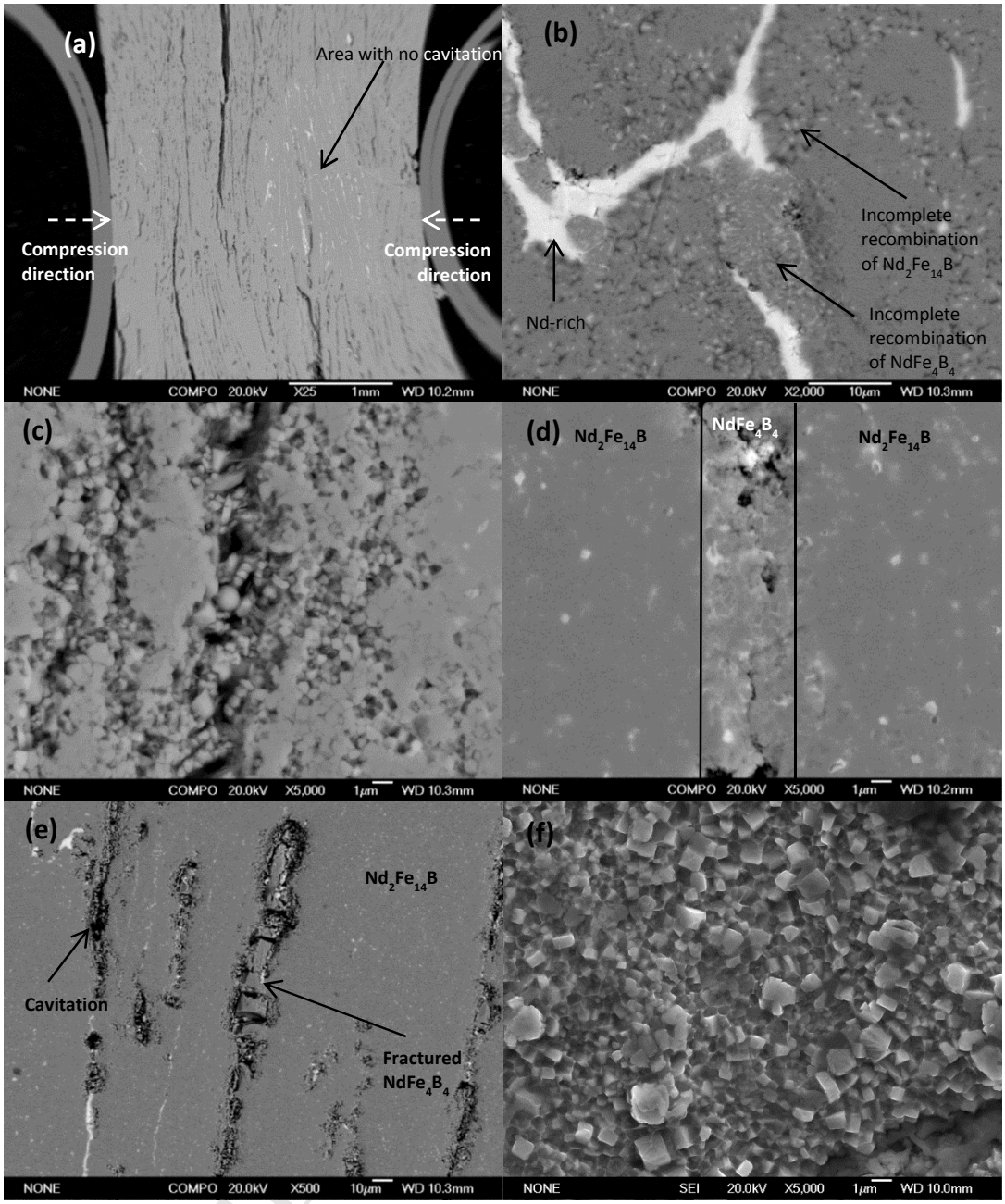

Figure 7 SEM images of the disproportionated pressed recombined VSM sample; (a) cross section, (b) cavitation in recombined sample, (c) incomplete recombination, (d) recombined $NdFe_4B_4$ phase, (e) fully recombined area and (f) a fractured surface of the recombined material.

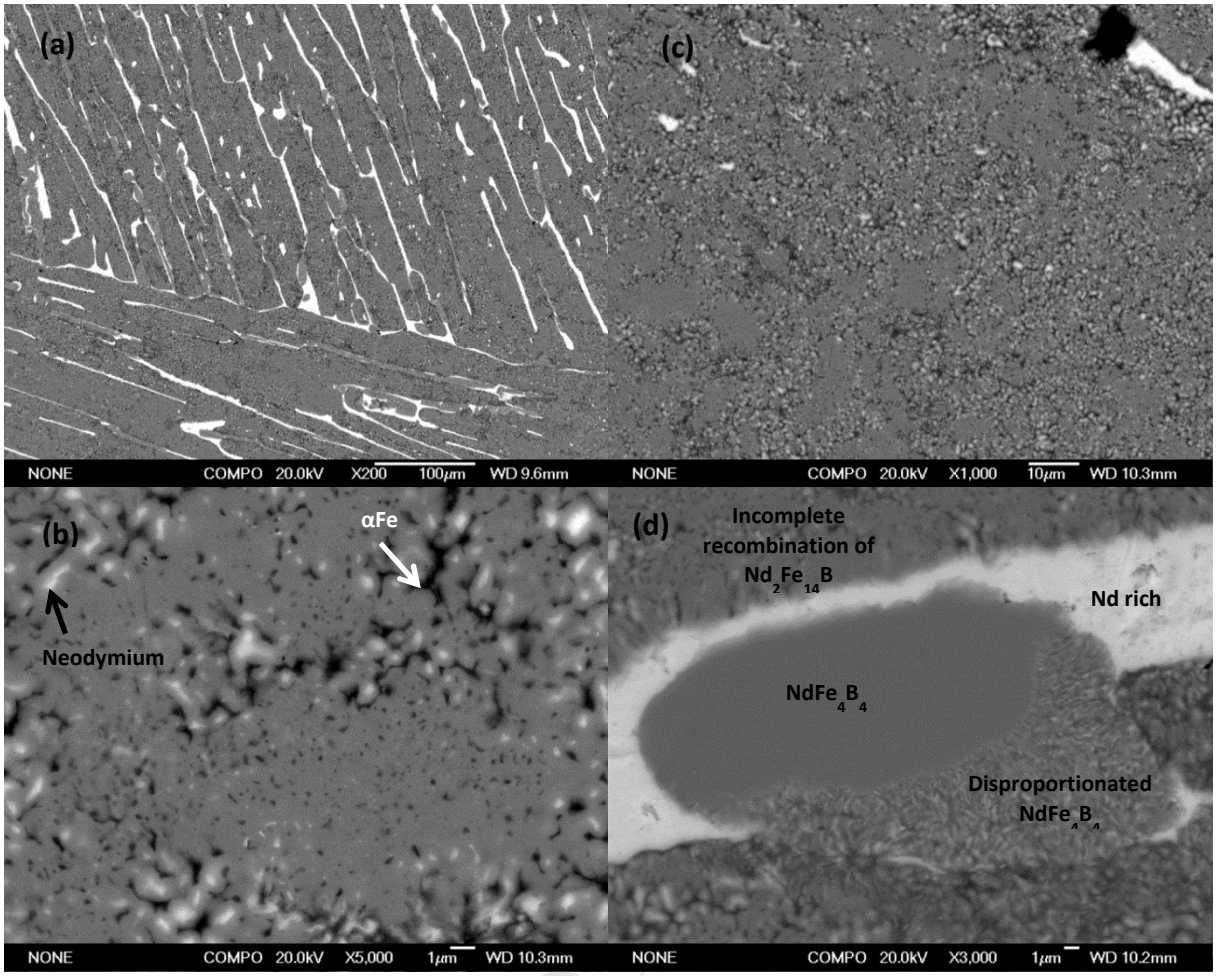

Figure 8 Backscattered SEM image of s-HDDR sample (without compression) used for the VSM measurements; (a) cross section, (b) incomplete recombined area, (c) incomplete recombination of $Nd_2Fe_{14}B$ area, and (d) incomplete recombination of $NdFe_4B_4$ area.

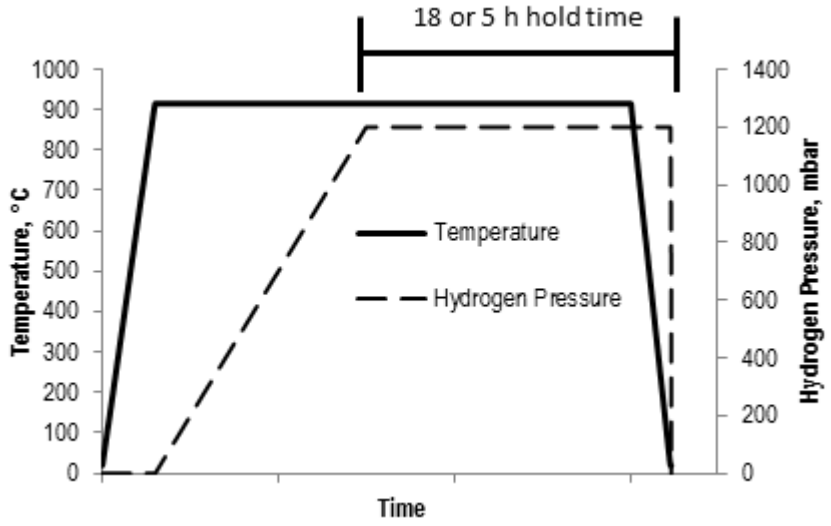

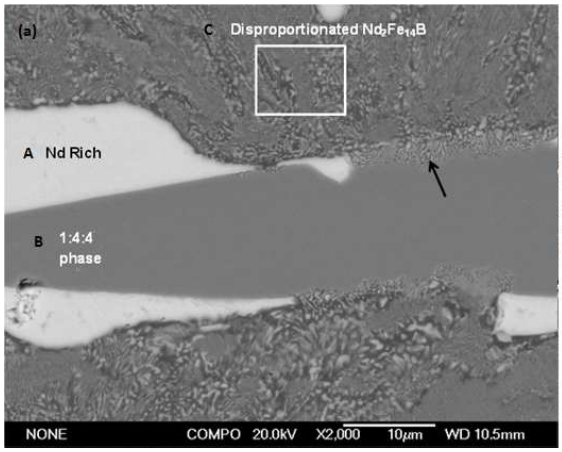

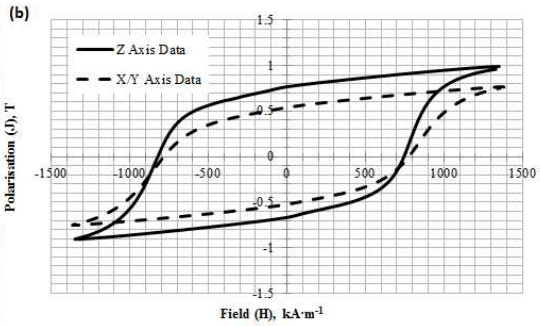

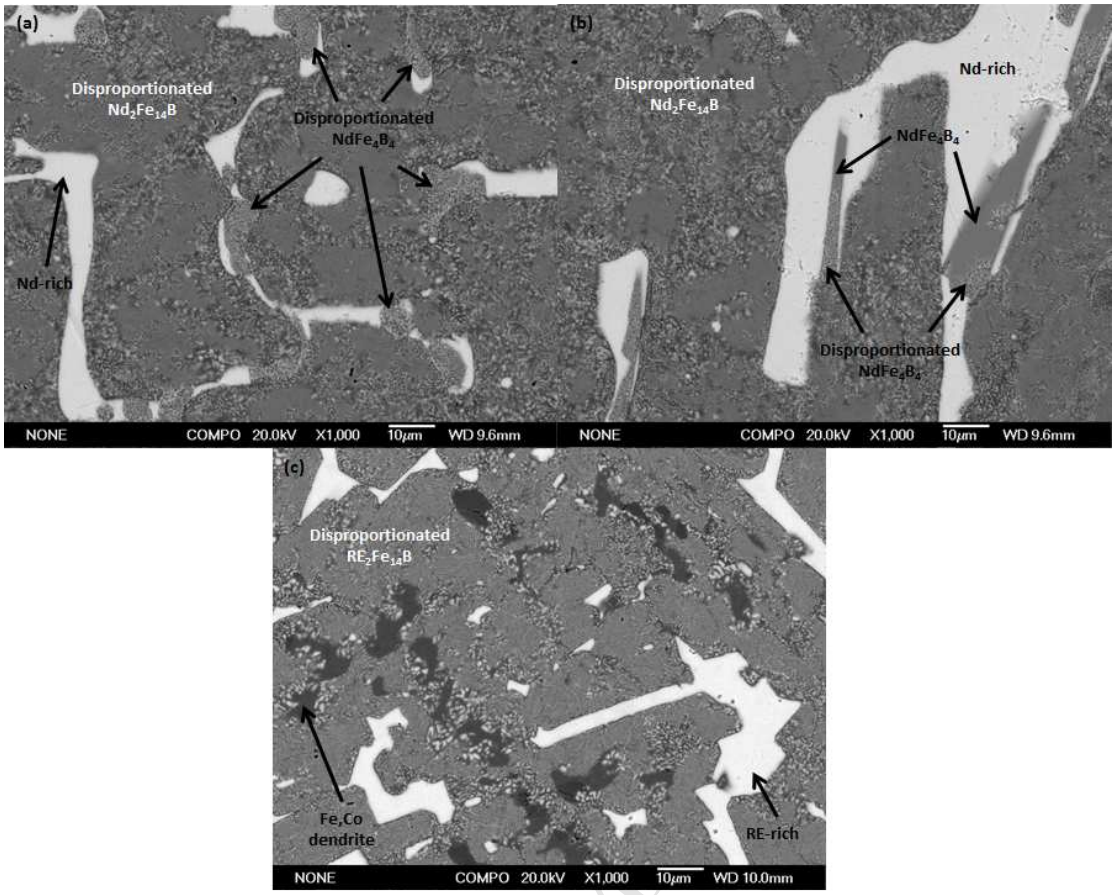

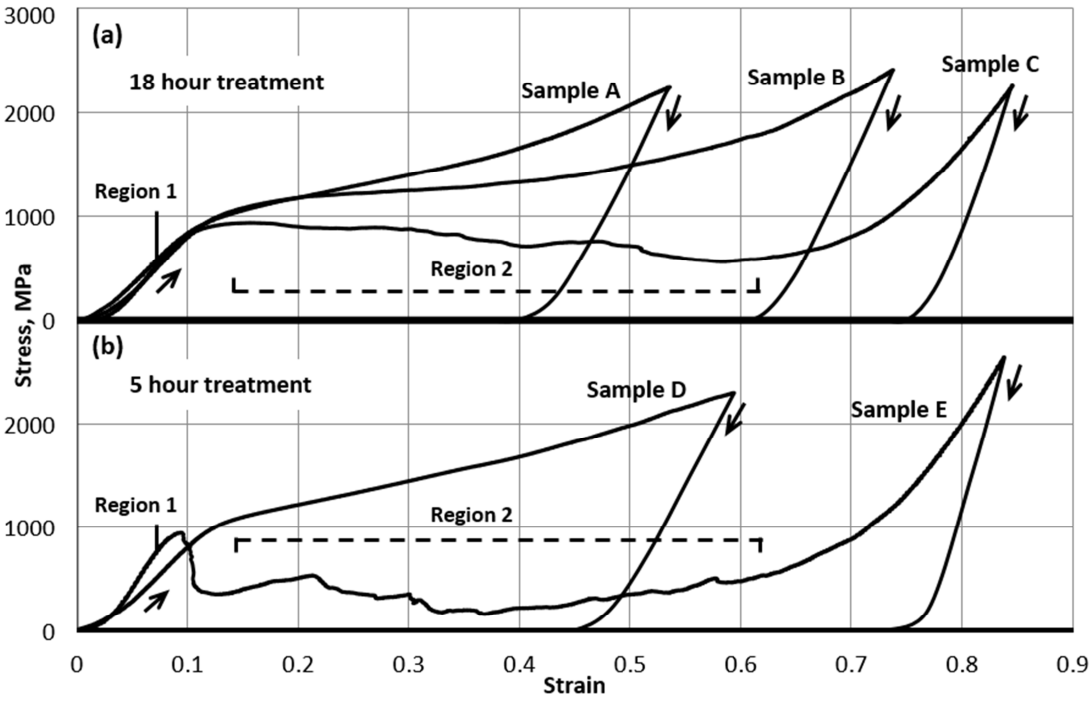

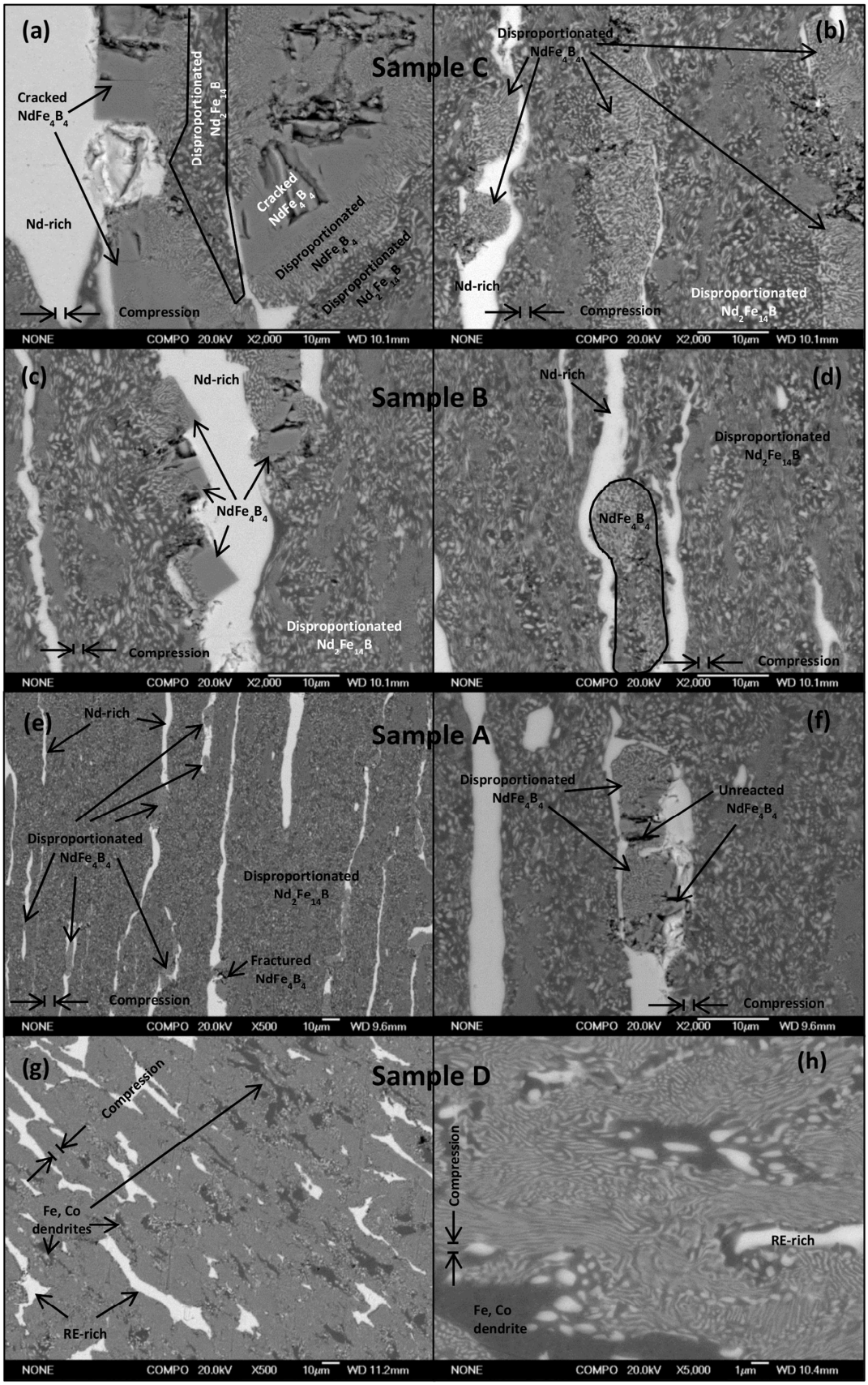
(a)
Sample C
Cracked $NdFe_4B_4$
Disproportionated $Nd_2Fe_{14}B$
Nd-rich
Cracked $NdFe_4B_4$
Disproportionated $NdFe_4B_4$
Disproportionated $Nd_2Fe_{14}B$
Compression
NONE COMPO 20.0kV X2,000 10μm WD 10.1mm
(b)
Disproportionated $NdFe_4B_4$
Nd-rich
Compression
Disproportionated $Nd_2Fe_{14}B$
NONE COMPO 20.0kV X2,000 10μm WD 10.1mm
(c)
Sample B
Nd-rich
$NdFe_4B_4$
Disproportionated $Nd_2Fe_{14}B$
Compression
NONE COMPO 20.0kV X2,000 10μm WD 10.1mm
(d)
Nd-rich
Disproportionated $Nd_2Fe_{14}B$
$NdFe_4B_4$
Compression
NONE COMPO 20.0kV X2,000 10μm WD 10.1mm
(e)
Sample A
Nd-rich
Disproportionated $NdFe_4B_4$
Disproportionated $Nd_2Fe_{14}B$
Fractured $NdFe_4B_4$
Compression
NONE COMPO 20.0kV X500 10μm WD 9.6mm
(f)
Disproportionated $NdFe_4B_4$
Unreacted $NdFe_4B_4$
Compression
NONE COMPO 20.0kV X2,000 10μm WD 9.6mm
(g)
Sample D
Compression
Fe, Co dendrites
RE-rich
NONE COMPO 20.0kV X500 10μm WD 11.2mm
(h)
Compression
RE-rich
Fe, Co dendrite
NONE COMPO 20.0kV X5,000 1μm WD 10.4mm

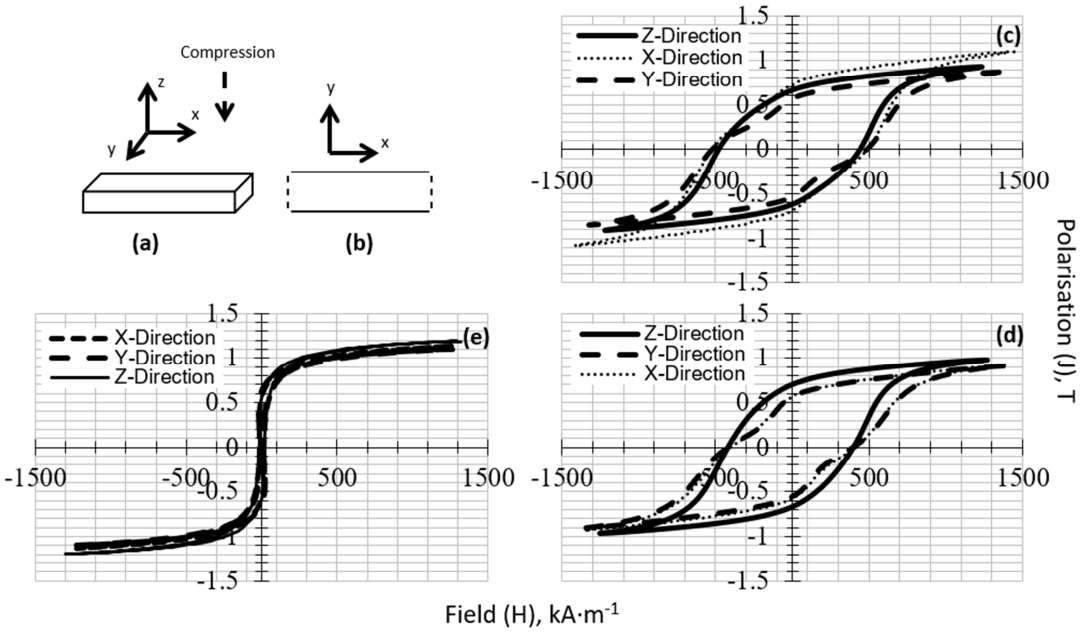

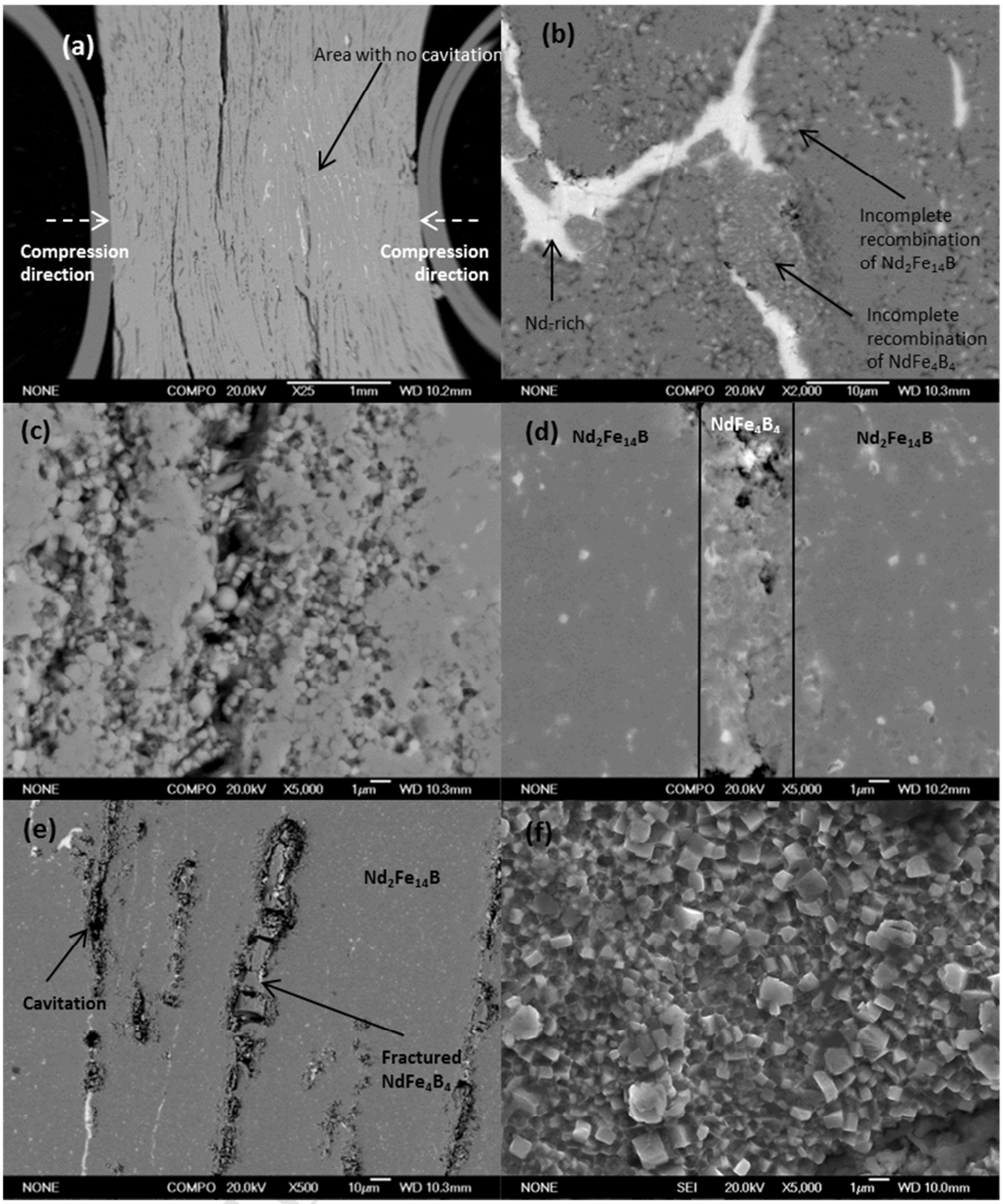
(a)
Area with no cavitation
Compression direction
Compression direction
NONE COMPO 20.0kV X25 1mm WD 10.2mm
(b)
Incomplete recombination of $Nd_2Fe_{14}B$
Nd-rich
Incomplete recombination of $NdFe_4B_4$
NONE COMPO 20.0kV X2,000 10μm WD 10.3mm
(c)
NONE COMPO 20.0kV X5,000 1μm WD 10.3mm
(d)
$Nd_2Fe_{14}B$
$NdFe_4B_4$
$Nd_2Fe_{14}B$
NONE COMPO 20.0kV X5,000 1μm WD 10.2mm
(e)
$Nd_2Fe_{14}B$
Cavitation
Fractured $NdFe_4B_4$
NONE COMPO 20.0kV X500 10μm WD 10.3mm
(f)
NONE SEI 20.0kV X5,000 1μm WD 10.0mm